79-4030

Observer Modal Control of Dual-Spin Flexible Spacecraft

L. Meirovitch* and H. Öz†
Virginia Polytechnic Institute and State University, Blacksburg, Va.

A procedure is presented for the control of a dual-spin spacecraft consisting of a spinning rigid rotor and a flexible despun section. Such a system exhibits gyroscopic effects. The system equations of motion are uncoupled by using gyroscopic modal analysis and the active control of the spacecraft is accomplished by synthesizing the control on the independent spacecraft modes. A deterministic (Luenberger-type) observer is designed by using decoupled dynamics and inserted in the control loop, where the control operates on an on-off scheme. Proportional control representing classical linear feedback approach is also discussed. Finally, the relation between spatially distributed actuators and modal control is discussed.

I. Introduction

THE new generation of large spacecraft calls for increased power, resulting in the inclusion of large flexible solar panels. On the other hand, the demand for increasingly precise attitude control has become a problem of major concern in a control system design. Although the fields of structural dynamics and modern control theory are both well developed, the problem of control of large flexible spacecraft, which requires a synthesis of both disciplines because of the interaction between flexibility and control systems, has only recently received serious attention. The problem is simply one of control of a distributed parameter system, a problem of high complexity.

Modal control of a linear dynamic system is not a new idea (see, for example, Ref. 1, Sec. 10.4). It essentially calls for the determination of a linear transformation for the system to reduce the simultaneous differential equations describing the system behavior to a set of independent (or nearly independent) equations. The input-output relations of the uncoupled (or nearly uncoupled) equations can be described conveniently by a block diagram in terms of transfer functions. The implementation of modal control for general systems has been very rare because of difficulty in producing the Jordan form. A different approach to the control problem consists of modifying the system eigenvalues and is also referred to as modal control.[2,3] Although the objectives in Refs. 2 and 3 are the same, the details are different. In both references, the eigenvalue modification is carried out without uncoupling. For a linear dynamic system defined by symmetric inertia and stiffness matrices, however, uncoupling of the system is relatively simple and computationally efficient. The procedure involves a coordinate transformation using the modal matrix which diagonalizes the inertia and stiffness matrices simultaneously.[4] This approach has been used to control nongyroscopic systems such as missiles.[5] In the case of gyroscopic systems, the classical modal matrix cannot diagonalize the gyroscopic matrix because the latter is skew symmetric. Quite recently, Meirovitch[6,7] has developed a modal analysis for gyroscopic systems whereby a $2n$-order system is decomposed into independent conjugate pairs of first-order differential equations the solution of which can be obtained readily. The method was used by Meirovitch et al.[8] to control a spinning flexible spacecraft by modal synthesis using both linear and nonlinear controls. Reference 8 also shows how the system can be controlled via a deterministic (Luenberger-type) observer using decoupled dynamics.

Modal control of a dynamic system provides a better physical understanding of the system dynamics and of the control system analysis and design. Indeed, modal control makes it possible to ascertain the degree of participation of each spacecraft mode in the overall system response. Perhaps more important is the fact that, because the uncoupled system consists of a set of n independent pairs of first-order equations, the techniques of analysis and design associated with second-order systems are applicable. For example, one can plot a phase diagram in the plane defined by a given pair of conjugate generalized coordinates, thus being able to implement nonlinear control and at the same time follow the progress toward regulation of each of the spacecraft modes. The pairs of uncoupled equations are identical in structure, so that the controller design has a modular form, consisting of an array of identical noninteracting units acting in parallel. The computational advantages of modal control become more pronounced as the order of the system increases. It suffices to point out that the method can be used for systems with several hundreds degrees of freedom. The price that one must pay for modal control is surprisingly low, and it amounts to the solution of the eigenvalue problem for the system. But, as demonstrated in Ref. 6, the eigenvalue problem for linear gyroscopic systems can be reduced to one in terms of a single real symmetric matrix, for which many stable, computationally efficient algorithms exist. The resulting Jordan form is a block-diagonal matrix, with 2×2 blocks consisting of the spacecraft natural frequencies multiplied by the matrix counterpart of $i=\sqrt{-1}$. This is in marked contrast to the reduction to Jordan form for general nonsymmetric matrices, which is not feasible for high-order systems.

In this paper, it is shown how the methods of Refs. 6-8 can be applied to the control of a dual-spin spacecraft consisting of a spinning rigid rotor with a flexible despun section. Results are presented for nonlinear control of the relay type and proportional control. Moreover, an observer for the system is constructed and control of the spacecraft is implemented via this observer for the relay-type control. In addition, phase plots for pairs of conjugate generalized coordinates are displayed for relay-type control. Also, the problem of spatial distribution of actuators is discussed. It should be pointed out that the method is restricted to undamped systems.

II. Modal Analysis for Gyroscopic Systems

We shall be concerned with the control of an undamped flexible spacecraft consisting of a given number of sub-

Presented at the AIAA Symposium on Dynamics and Control of Large Flexible Spacecraft, Blacksburg, Va., June 13-15, 1977; submitted July 20, 1977; revision received Sept. 5, 1978.

Index categories: Spacecraft Dynamics and Control; Structural Dynamics.

*Professor, Dept. of Engineering Science and Mechanics. Associate Fellow AIAA.

†Instructor, Dept. of Engineering Science and Mechanics.

structures. In the nominal equilibrium state, one of the substructures rotates with uniform angular velocity, whereas the rest of the structure is at rest relative to an inertial space. This implies that rigid body translations have been eliminated from the problem formulation. Under these circumstances, some of the generalized coordinates represent angular motions and the balance represent elastic displacements relative to suitable reference frames. In general, angular motions depend only on time, and elastic displacements depend on time and spatial positions. We shall assume that the structure has been discretized, so that all of the system generalized coordinates depend on time alone. Moreover, assuming that the rotating part possesses certain inertia (and possibly stiffness if the part is flexible) symmetry, the small motions from the nominal equilibrium can be described by the linear gyroscopic system of equations

$$m\ddot{q}(t)+g\dot{q}(t)+kq(t)=Q(t) \tag{1}$$

where m, g, and k are $n\times n$ mass, gyroscopic, and stiffness matrices, q is an n-dimensional configuration vector, and Q an n-dimensional generalized force vector. Note that q contains both angular and elastic coordinates and Q contains both torques and forces. The matrices m and k are assumed to be symmetric and positive definite and the matrix g is skew symmetric. The matrix g contains the Coriolis effects and the matrix k contains the centrifugal effects, in addition to the ordinary elastic effects.

A frequently encountered case is that in which no part of the spacecraft spins, in which case the gyroscopic matrix is zero, so that the system is nongyroscopic. In this case, the response can be obtained by the classical modal analysis, which is based on symmetric matrices. When g is not zero, i.e., in the gyroscopic case, the classical modal analysis breaks down, because the coordinate transformation which diagonalizes m and k simultaneously cannot possibly diagonalize g. A modal analysis for gyroscopic systems of the type in Eq. (1) has been developed recently by the first author of this paper (see Refs. 6 and 7). The method works with the $2n$-state vector $x=[\dot{q}T\,qT]T$ instead of the configuration vector. In the first place, it transforms the set of n second-order differential Eqs. (1) into the set of $2n$ first-order differential equations

$$M\dot{x}(t)+Gx(t)=X(t) \tag{2}$$

where

$$M=\begin{bmatrix} m & 0 \\ 0 & k \end{bmatrix} \quad G=\begin{bmatrix} g & k \\ -k & 0 \end{bmatrix} \quad X(t)=\begin{bmatrix} Q(t) \\ \mathbf{0} \end{bmatrix} \tag{3}$$

The eigenvalue problem associated with Eq. (2) possesses complex eigenvalues and eigenvectors. It is shown in Ref. 6 that the eigenvalue problem can be transformed into a problem in terms of real symmetric matrices having the eigenvalues ω_r^2 and the eigenvectors y_r and z_r $(r=1,2,\ldots,n)$. The eigenvalues ω_r^2 have multiplicity two, as to every eigenvalue belong the two eigenvectors y_r and z_r, which are the real and imaginary parts of the complex eigenvector x_r associated with Eq. (2), where the eigenvectors are orthogonal (and can be rendered orthonormal) with respect to the matrix M.

The set of orthonormal vectors y_r and $z_r(r=1,2,\ldots,n)$ constitute a basis in a $2n$-vector space. Hence, according to the expansion theorem,[7] any state vector $x(t)$ can be represented by a series of the form

$$x(t)=\sum_{r=1}^{n}[\xi_r(t)y_r+\eta_r(t)z_r] \tag{4}$$

where $\xi_r(t)$ and $\eta_r(t)$ are generalized coordinates associated with the modal vectors y_r and z_r, respectively. Introducing Eq. (4) into Eq. (2), multiplying the result by y_s and z_s in sequence, and taking advantage of the orthogonality of the eigenvectors, we obtain the set of n independent equations:

$$\begin{aligned} &\dot{\xi}_r(t)-\omega_r\eta_r(t)=Y_r(t) \\ &\dot{\eta}_r(t)+\omega_r\xi_r(t)=Z_r(t) \end{aligned} \qquad (r=1,2,\ldots,n) \tag{5}$$

where

$$Y_r(t)=y_r^{\mathrm{T}}X(t) \qquad Z_r(t)=z_r^{\mathrm{T}}X(T) \quad (r=1,2,\ldots,n) \tag{6}$$

are generalized forces. Equations (5) for the pair of generalized coordinates $\xi_r(t)$ and $\eta_r(t)$ can be solved independently of the equations for any other pair.

The preceding decoupling procedure can be cast into matrix form by introducing the $2n$-dimensional uncoupled state vector

$$w=[\xi_1\ \eta_1\ \xi_2\ \eta_2\ldots\xi_n\ \eta_n]^{\mathrm{T}} \tag{7}$$

and the corresponding $2n\times 2n$ modal matrix

$$P=[y_1\ z_1\ y_2\ z_2\ldots y_n\ z_n] \tag{8}$$

Then, the expansion theorem, Eq. (4), becomes simply

$$x(t)=Pw(t) \tag{9}$$

Moreover, the orthogonality relations can be shown to have the compact form

$$P^{\mathrm{T}}MP=I_{2n} \qquad P^{\mathrm{T}}GP=-A \tag{10}$$

where I_{2n} is a unit matrix of order $2n$ and A is a block-diagonal matrix of the form

$$A=\begin{bmatrix} \omega_1 i & 0 & \ldots & 0 \\ 0 & \omega_2 i & \ldots & 0 \\ \ldots & \ldots & \ldots & \ldots \\ 0 & 0 & \ldots & \omega_n i \end{bmatrix} \qquad i=\begin{bmatrix} 0 & 1 \\ -1 & 0 \end{bmatrix} \tag{11}$$

The matrix counterpart of Eqs. (5) is simply

$$\dot{w}=Aw+P^{\mathrm{T}}X \tag{12}$$

For future reference, we note that

$$w(t)=P^{\mathrm{T}}Mx(t) \tag{13}$$

The preceding uncoupling procedure is valid only for undamped systems, because in the case of damping it is not possible to construct matrices M and G [Eqs. (3)] with the desired properties.

III. Control of Gyroscopic Systems by Modal Synthesis

The modal analysis presented in Sec. II can be used to control a gyroscopic system. The method for controlling a gyroscopic system by modal synthesis has been developed in a recent paper by Meirovitch et al.[8] The advantage of the method lies in the fact that it can treat linear gyroscopic systems of large order, such as those associated with flexible spacecraft. In this section we shall review briefly the main results obtained in Ref. 8.

Letting the external excitation be equal to zero and denoting by $U(t)$ the control vector, the system differential equations

of motion can be written in the form

$$M\dot{x}(t)+Gx(t)=U(t) \tag{14}$$

which are subject to the initial excitation $x(0)$. The problem is that of designing a control system, i.e., of constructing a vector $U(t)$ which will reduce the oscillation to zero (regulator problem) or to reduce it to a tolerable level. Using the decoupling procedure of Sec. II, Eq. (14) can be reduced to the form (5), in which

$$Y_r(t)=y_r^{\mathrm{T}}U(t) \quad Z_r(t)=z_r^{\mathrm{T}}U(t) \qquad (r=1,2,\ldots,n) \tag{15}$$

One control scheme is the proportional control given by

$$Y_r(t)=0 \qquad Z_r(t)=-2\zeta_r\omega_r\eta_r(t) \qquad (r=1,2,\ldots,n) \tag{16}$$

which can be interpreted as artificial damping. In this case, the uncoupled response is

$$\xi_r(t)=e^{-\zeta_r\omega_r t}\left[\xi_r(0)\cos\omega_{dr}t+\frac{\zeta_r\xi_r(0)+\eta_r(0)}{(1-\zeta_r^2)^{1/2}}\sin\omega_{dr}t\right]$$

$$\eta_r(t)=e^{-\zeta_r\omega_r t}\left[\eta_r(0)\cos\omega_{dr}t-\frac{\zeta_r\eta_r(0)+\xi_r(0)}{(1-\zeta_r^2)^{1/2}}\sin\omega_{dr}t\right]$$

$$(r=1,2,\ldots,n) \tag{17}$$

where $\omega_{dr}=(1-\zeta_r^2)^{1/2}\omega_r$. The response represents oscillation decaying exponentially.

An undesirable feature of proportional control is that it must operate continuously. A scheme which does not have this drawback is on-off control with deadband. The deadband implies that some low-amplitude oscillation is acceptable. In this case, the decoupled conjugate control forces are

$$Y_r(t)=0 \qquad Z_r(t)=u_r/\omega_r \qquad (r=1,2,\ldots,n) \tag{18}$$

where u_r is a nonlinear function of η_r given explicitly by

$$u_r=\begin{cases}-k_r & (\eta_r>d_r)\\ 0 & (|\eta_r|\le d_r)\\ k_r & (\eta_r<-d_r)\end{cases} \tag{19}$$

where d_r is a constant depending on the tolerable amplitude of oscillation. The solutions are as follows.

For $|\eta_r|\le d_r$:

$$\xi_r(t)=\xi_r(0)\cos\omega_r t+\eta_r(0)\sin\omega_r t$$

$$\eta_r(t)=-\xi_r(0)\sin\omega_r t+\eta_r(0)\cos\omega_r t \qquad (r=1,2,\ldots,n) \tag{20a}$$

For $\eta_r>d_r$:

$$\xi_r(t)=-k_r/\omega_r^2+[\xi_r(0)+k_r/\omega_r^2]\cos\omega_r t+\eta_r(0)\sin\omega_r t$$

$$\eta_r(t)=-[\xi_r(0)+k_r/\omega_r^2]\sin\omega_r t+\eta_r(0)\cos\omega_r t$$

$$(r=1,2,\ldots,n) \tag{20b}$$

For $\eta_r<-d_r$:

$$\xi_r(t)=k_r/\omega_r^2+[\xi_r(0)-k_r/\omega_r^2]\cos\omega_r t+\eta_r(0)\sin\omega_r t$$

$$\eta_r(t)=-[\xi_r(0)-k_r/\omega_r^2]\sin\omega_r t+\eta_r(0)\cos\omega_r t$$

$$(r=1,2,\ldots,n) \tag{20c}$$

Both solutions (17) and (20) can be displayed conveniently in the form of phase-plane plots η_r vs ξ_r. There remains the question of the actual control implementation. This question is addressed specifically in Ref. 9.

IV. Reconstruction of the State Vector by Means of a Deterministic Observer

The two control schemes discussed in Sec. III are predicated on the knowledge of the state of the system at any time. Indeed, according to Eqs. (16) and (18), the control force $Z_r(t)$ depends on the generalized coordinate $\eta_r(t)$ $(r=1,2,\ldots,n)$, in the first scheme linearly and in the second scheme nonlinearly. In most cases, however, the state vector is not completely known, so that it is necessary to estimate it. To this end, it is often possible to construct another dynamical system which is closely related to the actual system and is capable of approximating the behavior of the actual system. Such a dynamical system is known as an observer. Deterministic observers were first proposed by Luenberger.[10]

The equations of motion of a controlled spacecraft subjected to external excitation can be written in the form

$$M\dot{x}+Gx=X+U \tag{21}$$

where X is a vector of known excitations from external sources, such as solar radiation pressure, and U is the control vector. Following the procedure of Sec. II, the decoupled equations of motion can be written as

$$\dot{w}=Aw+P^{\mathrm{T}}(X+U) \tag{22}$$

where w, A, and P are as defined in Sec. II.

The observer design can be best brought about by using the uncoupled dynamical system, Eq. (22). Generally, the control vector U is a function of the decoupled state vector w, where the latter is not available. To estimate the state vector, let us consider a vector of measurements $\dot{z}$ corresponding to the rate $\dot{w}$ of the state vector. Reference 11 contains a more detailed description of the nature of the measurements. We shall not go into the details here, but merely state the basic results of Ref. 11. Let the relation between the vectors $\dot{z}$ and $\dot{w}$ be

$$\dot{z}=C\dot{w} \tag{23}$$

where in general C is a constant $m\times 2n$ rectangular matrix, $m\le 2n$, which implies that the measurement vector $\dot{z}$ is not complete. Then, the object is to construct an observer to estimate the state vector by using the measurement vector $\dot{z}$ and the input vector $X+U$. It is assumed that there is no noise associated with the measurement process or that, if there is noise, the noise-to-signal ratio is sufficiently small that a deterministic observer can be used. Denoting the estimated state vector by $\hat{w}(t)$, it is shown in Ref. 8 that the observer can be described by the differential equation

$$\dot{\hat{w}}=A_0\hat{w}+B_0\dot{z}+N_0P^{\mathrm{T}}(X+U) \tag{24}$$

where B_0 is a $2n\times m$ rectangular matrix. Using Eq. (23), Eq. (24) can be written in the form

$$\dot{\hat{w}}=A_0\hat{w}+B_0^*\dot{w}+N_0P^{\mathrm{T}}(X+U) \tag{25}$$

where

$$B_0^*=B_0C \tag{26}$$

is a square matrix of order $2n$. It is shown in Ref. 8 that if the matrices A_0, B_0^*, and N_0 satisfy

$$A_0=(I-B_0^*)A=(I-B_0C)A \tag{27a}$$

$$N_0=I-B_0^*=I-B_0C \tag{27b}$$

the difference $w(t)-\hat{w}(t)$ between the actual and the reconstructed state vectors, known as the estimation error $\epsilon(t)$, satisfies

$$\dot{\epsilon}(t)=A_0\epsilon(t) \tag{28}$$

The vector $\dot{w}$ appearing in Eq. (25) can be regarded as the rate measurement vector $\dot{w}_m$, although in reality we do not require a complete set of $2n$ measurements. Moreover, it should be recognized that the sensors do not actually measure the uncoupled generalized velocity vector $\dot{w}$, nor the coupled vector $\dot{x}$, but they measure nutation rates and elastic velocities, as inferred from signals generated by sensors distributed throughout the spacecraft. In view of this, we conclude that the observer described in Eq. (24) will estimate the state vector provided $\epsilon(t)\to\mathbf{0}$ as $t\to\infty$. Introducing Eqs. (26) and (27) into Eq. (25), the observer dynamics can be shown to be equivalent to

$$\dot{\hat{w}}=A\hat{w}+B_0(\dot{z}-\dot{\hat{z}})+P^{\mathrm{T}}(X+U) \tag{29}$$

where

$$\dot{\hat{z}}=C\dot{\hat{w}}=C[A\hat{w}+P^{\mathrm{T}}(X+U)] \tag{30}$$

The second term on the right side of Eq. (29) is known as the measurement residual. Equation (29) represents a decoupled observer for the pair of generalized coordinates ξ_r, η_r $(r=1,2,\ldots,n)$, because the matrix A is block-diagonal with 2×2 blocks on the diagonal. The excitation vector for the observer is given by the last two terms on the right side of Eq. (29), i.e,

$$\hat{Q}=B_0(\dot{z}-\dot{\hat{z}})+P^{\mathrm{T}}(X+U) \tag{31}$$

Equation (31) can be written in the form

$$\hat{Q}=\hat{Q}_z+\hat{Q}_X+\hat{Q}_U \tag{32}$$

where

$$\hat{Q}_z=B_0(\dot{z}-\dot{\hat{z}}) \qquad \hat{Q}_X=P^{\mathrm{T}}X \qquad \hat{Q}_U=P^{\mathrm{T}}U \tag{33}$$

The vector $\hat{Q}_z$ depends on time explicitly through the measurement residual vector. On the other hand, $\hat{Q}_U$ has the form

$$\hat{Q}_U=[0 \quad u_1/\omega_1 \quad 0 \quad u_2/\omega_2 \quad \ldots \quad u_n/\omega_n]^{\mathrm{T}} \tag{34}$$

where $u_r(r=1,2,\ldots,n)$ are the relay-type functions given by Eqs. (19), so that $\hat{Q}_U$ depends on time only implicitly. In a computer simulation, however, the components of the vector $\hat{Q}_U$ are evaluated at discrete values of time, so that in effect the vector can be regarded as depending explicitly on time. On the other hand, the vector $\hat{Q}_X$ reflects the effect of external disturbances on the spacecraft. This permits us to write the following equation for the uncoupled observer

$$\dot{\hat{w}}(t)=A\hat{w}(t)+\hat{Q}(t) \tag{35}$$

which has the solution

$$\hat{w}(t)=e^{tA}\hat{w}(0)+\int_0^t e^{(t-\tau)A}\hat{Q}(\tau)\,\mathrm{d}\tau \tag{36}$$

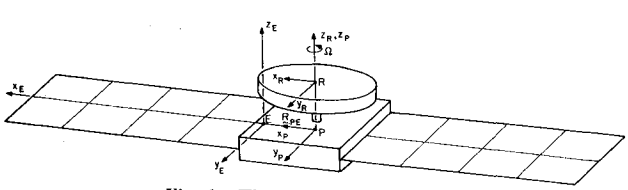

Fig. 1 The dual-spin spacecraft.

The behavior of the observer state vector $\hat{w}(t)$ is better understood by considering the alternative form of the observer dynamics, namely Eq. (24), whose solution is

$$\hat{w}(t)=e^{tA_0}\hat{w}(0)+\int_0^t e^{(t-\tau)A_0}\{B_0\dot{z}(\tau)+N_0P^{\mathrm{T}}[X(\tau)+U(\tau)]\}\mathrm{d}\tau \tag{37}$$

If the gain matrix B_0 is chosen such that the observer matrix A_0 in Eq. (27a) has eigenvalues with negative real parts, then we conclude from Eq. (28) that the error vector $\epsilon(t)$ approaches zero as $t\to\infty$, and the observer response will only depend on the convolution integral in Eq. (37). Note that the first term on the right side of Eq. (37) will vanish regardless of the initial state of the observer, from which we conclude that this state can be chosen arbitrarily. Finally, the coupled observer state vector $\hat{x}(t)$ can be obtained from the uncoupled one from the equation

$$\hat{x}(t)=P\hat{w}(t) \tag{38}$$

In the foregoing, we presented a procedure for the design of a decoupled full-order observer. Given m independent system outputs, however, it is possible to design a reduced observer of order $2n-m$.[10] As the emphasis here is on the question of decoupled vs coupled observers and not reduced-order vs full-order observers, we shall not pursue the latter subject here. The design of a reduced-order observer for a flexible gyroscopic system is presented in Ref. 9.

V. Spatial Distribution of Control Forces and Torques

The control forces and torques introduced in Sec. III were in essence discrete quantities associated with the corresponding generalized coordinates. The question as to how the discretized generalized control force vector was derived, which is an important question in actual control implementation, was left open. In the design of a controller for a distributed system, such as a flexible spacecraft, the control forces and torques are generally distributed throughout the structure, so that it is necessary to specify first their spatial location and then to derive the discretized counterparts. In general, the performance of a control system depends on the spatial location of the actuators and an optimal design involves, among other things, choosing the "best" location consistent with some desired spacecraft performance. In this paper, we shall not concern ourselves with the optimization problem but merely with the derivation of the mathematical relations making the transition between the physical distributed controls and the more abstract discretized generalized controls.

Let a given number of control torques $M_i(i=1,2,\ldots,k)$ and control forces $F_j(j=1,2,\ldots,l)$ be acting throughout the structure, concentrated at given points $P=P_i$ and $P=P_j$, respectively. These torques and forces can be represented as distributed torques and forces by writing them in the form $M_i\delta(P-P_i)$ and $F_j\delta(P-P_j)$ where $\delta(P-P_i)$ and $\delta(P-P_j)$ are spatial delta functions. We shall assume that the torques operate on rigid parts of the spacecraft and the forces on elastic parts, so that in effect the torques are designed to control rigid body rotations primarily and the forces elastic displacements primarily.

Next, let us denote the virtual rotation vector by $\partial\boldsymbol{\theta}$ and the virtual displacement vector of an arbitrary point of the elastic member by $\delta\boldsymbol{R}_E$, where

$$\delta\boldsymbol{R}_E=[\tilde{R}_{PE}+\tilde{r}_E+\tilde{u}_E]^{\mathrm{T}}\delta\boldsymbol{\theta}+\delta\boldsymbol{u}_E \tag{39}$$

in which $\boldsymbol{R}_{PE}$ denotes the vector from P to E, $\boldsymbol{r}_E$ the nominal position of a point in the elastic member, and $\boldsymbol{u}_E$ the elastic

displacement of the point (see Fig. 1). For any vector r, the notation $\tilde{r}$ implies the skew symmetric matrix

$$\tilde{r}=\begin{bmatrix} 0 & -z & y \\ z & 0 & -x \\ -y & x & 0 \end{bmatrix} \tag{40}$$

where x, y, z are the components of the vector r. Hence, the virtual work due to control torques and forces is

$$\delta W_c=\int_{S_R} \boldsymbol{M}_i^{\mathrm{T}}\delta(P-P_i)\delta\boldsymbol{\theta}\,\mathrm{d}S_R+\int_{S_E}\boldsymbol{F}_j^{\mathrm{T}}\delta(P-P_j)\delta\boldsymbol{R}_E\,\mathrm{d}S_E$$

$$=\sum_{i=1}^{k}\boldsymbol{M}_i^{\mathrm{T}}(P_i,t)\delta\boldsymbol{\theta}(t)+\sum_{j=1}^{l}\boldsymbol{F}_j^{\mathrm{T}}(P_j,t)\,[\tilde{R}_{PE}+\tilde{r}_E(P_j)$$

$$+\tilde{u}_E(P_j,t)\,]^{\mathrm{T}}\delta\boldsymbol{\theta}(t)+\delta\boldsymbol{u}_E(P_j,t)\cong\sum_{i=1}^{k}\boldsymbol{M}_i^{\mathrm{T}}(P_i,t)\delta\boldsymbol{\theta}(t)$$

$$+\sum_{j=1}^{l}\boldsymbol{F}_j^{\mathrm{T}}(P_j,t)\,[\tilde{R}_{PE}+\tilde{r}_E(P_j)\,]^{\mathrm{T}}\delta\boldsymbol{\theta}(t)+\sum_{j=1}^{l}\boldsymbol{F}_j^{\mathrm{T}}(P_j,t)\delta\boldsymbol{u}_E(P_j,t) \tag{41}$$

where the term $\tilde{u}_E^{\mathrm{T}}(P_j,t)\delta\boldsymbol{\theta}(t)$ was ignored as being of higher order.

With reference to Fig. 1, we shall assume that the torque vector has no component in the z direction and that the force vector has no component in the x direction, or

$$\boldsymbol{M}_i=[M_{xi}\quad M_{yi}\quad 0]^{\mathrm{T}}\qquad \boldsymbol{F}_j=[F_{yj}\quad F_{zj}]^{\mathrm{T}} \tag{42}$$

$$[\tilde{R}_{PE}+\tilde{r}_E(P_j)\,]^{\mathrm{T}}=\begin{bmatrix} 0 & 0 & -y_{Pj} \\ 0 & 0 & R+x_{Pj} \\ y_{Pj} & -(R+x_{Pj}) & 0 \end{bmatrix} \tag{43}$$

Introducing Eqs. (42) and (43) into Eq. (41), we obtain

$$\delta W_c=\Big[\sum_{i=1}^{k}M_{xi}(P_i,t)+\sum_{j=1}^{l}y_{pj}F_{zj}(P_j,t)\Big]\delta\theta_1$$

$$+\Big[\sum_{i=1}^{k}M_{yi}(P_i,t)-\sum_{j=1}^{l}(R+x_{Pj})F_{zj}(P_j,t)\Big]\delta\theta_2$$

$$+\sum_{j=1}^{l}(R+x_{Pj})F_{yj}(P_j,t)\delta\theta_3+\sum_{j=1}^{l}F_{yj}(P_j,t)\delta u_y(P_j,t)$$

$$+\sum_{j=1}^{l}F_{zj}(P_j,t)\delta u_z(P_j,t) \tag{44}$$

where $\delta\theta_1$, $\delta\theta_2$, and $\delta\theta_3$ are the components of $\delta\boldsymbol{\theta}$ and δu_y and δu_z the components of $\delta\boldsymbol{u}_E$; the component δu_x was assumed to be zero.

Next, let us introduce the discretization

$$\delta u_y=\boldsymbol{\phi}_y^{\mathrm{T}}\delta\zeta\qquad \delta u_z=\boldsymbol{\phi}_z^{\mathrm{T}}\delta\zeta \tag{45}$$

so that Eq. (44) becomes

$$\delta W_c=\Big[\sum_{i=1}^{k}M_{xi}(P_i,t)+\sum_{j=1}^{l}y_{Pj}F_{zj}(P_j,t)\Big]\delta\theta_1$$

$$+\Big[\sum_{i=1}^{k}M_{yi}(P_i,t)-\sum_{i=1}^{l}(R+x_{Pj})F_{zj}(P_j,t)\Big]\delta\theta_2$$

$$+\sum_{j=1}^{l}(R+x_{Pj})F_{yj}(P_j,t)\delta\theta_3$$

$$+\sum_{j=1}^{l}[F_{yj}(P_j,t)\boldsymbol{\phi}_y^{\mathrm{T}}(P_j)+F_{zj}(P_j,t)\boldsymbol{\phi}_z^{\mathrm{T}}(P_j)\,]\delta\zeta \tag{46}$$

In the system of Fig. 1, however, θ_3 is an ignorable coordinate. In fact, it will be shown in the next section that $\delta\theta_3$ satisfies

$$\delta\theta_3=-\frac{1}{C}\int_{m_E}(R+x)\delta u_y\,\mathrm{d}m_E=\boldsymbol{a}_y^{\mathrm{T}}\delta\zeta \tag{47}$$

where

$$\boldsymbol{a}_y^{\mathrm{T}}=-\frac{1}{C}\int_{m_e}(R+x)\boldsymbol{\phi}_y^{\mathrm{T}}\mathrm{d}m_E \tag{48}$$

Introducing Eq. (48) into Eq. (47), we can write

$$\delta W_c=Q_{\theta 1}\delta\theta_1+Q_{\theta 2}\delta\theta_2+\boldsymbol{Q}_\zeta^{\mathrm{T}}\delta\zeta \tag{49}$$

where

$$Q_{\theta 1}=\sum_{i=1}^{k}M_{xi}(P_i,t)+\sum_{j=1}^{l}y_{Pj}F_{zj}(P_j,t) \tag{50a}$$

$$Q_{\theta 2}=\sum_{i=1}^{k}M_{yi}(P_i,t)-\sum_{j=1}^{l}(R+x_{Pj})F_{zj}(P_j,t) \tag{50b}$$

$$\boldsymbol{Q}^{\mathrm{T}}=\sum_{j=1}^{l}[\,(R+x_{Pj})F_{yj}(P_j,t)\boldsymbol{a}_y^{\mathrm{T}}$$

$$+F_{yj}(P_j,t)\boldsymbol{\phi}_y^{\mathrm{T}}(P_j)+F_{zj}(P_j,t)\boldsymbol{\phi}_z^{\mathrm{T}}(P_j)\,] \tag{50c}$$

are the discretized generalized control forces, expressed in terms of the actual distributed control torques and forces. In terms of the notation of Sec. IV, we have

$$\boldsymbol{U}=[Q_{\theta 1}\quad Q_{\theta 2}\quad \boldsymbol{Q}_\zeta^{\mathrm{T}}\quad \boldsymbol{0}^{\mathrm{T}}]^{\mathrm{T}} \tag{51}$$

Equations (50) relate the discretized generalized control vector $\boldsymbol{U}$ to the actual control forces and torques. It should be recognized from Eqs. (50), however, that there is no one-to-one correspondence between the dimension of the generalized control vector $\boldsymbol{U}$ and the number of the physical actuators. Indeed, one actuator can yield a full vector $\boldsymbol{U}$, although the components of this vector will not be independent. Hence, in principle a single actuator can control the entire system, but the question remains as to how good a job it can do. Moreover, the components of $\boldsymbol{U}$ clearly depend on the location of the actuators. In fact, there is some arbitrariness in the selection of the number of actuators and their location through the spacecraft, so that the same vector $\boldsymbol{U}$ may be realized in different ways. This points to a new aspect of the problem, namely, control optimization with respect to the number and location of the actuators.

VI. Dual-Spin Spacecraft with Flexible Despun Section

Let us consider a dual-spin spacecraft consisting of a rigid platform with symmetric elastic panels and a rigid symmetric rotor spinning about an axis normal to the platform (Fig. 1). The spacecraft can be regarded as representing a simple mathematical model of a geostationary communications satellite or of a solar power satellite. In the nominal equilibrium state, the platform and the panels are at rest relative to an inertial space and the rotor spins with the constant angular velocity Ω relative to that space. When perturbed slightly, the rigid platform, and hence the rotor spin axis, acquires the small angular velocity components $\dot{\theta}_1$, $\dot{\theta}_2$, $\dot{\theta}_3$ about axes x, y, z, respectively, and every point of the panels acquires the elastic displacement $\boldsymbol{u}_E=[0\ u_y\ u_z]^{\mathrm{T}}$ relative to axes $x_Ey_Ez_E$. It is important to recognize that, because of the angular perturbations θ_1, θ_2, θ_3, the rotor axis will undergo some slight angular motion relative to its initial fixed orientation in space.

The dual-spin spacecraft just described can be regarded as a special case of the more general spacecraft treated in Ref. 8. Indeed, for the spacecraft at hand, if we use Eq. (9) of Ref. 8, then the kinetic energy reduces to

$$T=\frac{1}{2}\Omega_P^T J\Omega_P+\frac{1}{2}\omega_R^T J\omega_P+\Omega_P^T J_R\omega_r+\frac{1}{2}\int_{m_E}\dot{u}_E^T\dot{u}_E\,dm_E$$
$$+\Omega_P^T R_{PE}^T\tilde{r}_{EG}\Omega_P-\Omega_P^T\tilde{R}_{PE}^T p_E-\Omega_P^T h_E \tag{52}$$

where

$$\Omega_P=\begin{bmatrix}c\theta_3 & c\theta_1 s\theta_3 & 0\\ -s\theta_3 & c\theta_1 c\theta_3 & 0\\ 0 & -s\theta_1 & 1\end{bmatrix}\begin{bmatrix}\dot{\theta}_1\\ \dot{\theta}_2\\ \dot{\theta}_3\end{bmatrix}\quad \omega_R=\Omega\begin{bmatrix}s\theta_1 s\theta_3-c\theta_1 s\theta_2 c\theta_3\\ s\theta_1 c\theta_3+c\theta_1 s\theta_2 s\theta_3\\ c\theta_1 c\theta_2\end{bmatrix} \tag{53}$$

are the angular velocity vector of the platform and the angular velocity vector of the rotor relative to the platform, respectively, both expressed in terms of components along the platform axes. Moreover,

$$J=\begin{bmatrix}A & 0 & 0\\ 0 & B & 0\\ 0 & 0 & C\end{bmatrix}\quad J_R=\begin{bmatrix}A_R & 0 & 0\\ 0 & A_R & 0\\ 0 & 0 & C_R\end{bmatrix} \tag{54}$$

are inertia matrices of the entire spacecraft and of the rotor, where in anticipation of linearization deformation effects have been neglected in J. Other quantities appearing in Eq. (52) are

$$\tilde{R}_{PE}=\begin{bmatrix}0 & 0 & 0\\ 0 & 0 & -R\\ 0 & R & 0\end{bmatrix}\quad \tilde{r}_{EG}=\begin{bmatrix}0 & -\int u_z\,dm_E & \int u_y\,dm_E\\ \int u_z\,dm_E & 0 & 0\\ -\int u_y\,dm_E & 0 & 0\end{bmatrix} \tag{55}$$

and

$$\dot{u}_E=\begin{bmatrix}0\\ \dot{u}_y\\ \dot{u}_z\end{bmatrix}\quad p_E=\begin{bmatrix}0\\ \int\dot{u}_y\,dm_E\\ \int\dot{u}_z\,dm_E\end{bmatrix}\quad h_E=\begin{bmatrix}-\int y\dot{u}_z\,dm_E\\ \int x\dot{u}_z\,dm_E\\ -\int x\dot{u}_y\,dm_E\end{bmatrix} \tag{56}$$

Introducing Eqs. (53-56) into Eq. (52) and ignoring higher-order terms, the kinetic energy reduces to

$$T=\tfrac{1}{2}(A\dot{\theta}_1^2+B\dot{\theta}_2^2+C\dot{\theta}_3^2)+\tfrac{1}{2}\Omega^2(A_R-C_R)(\theta_1^2+\theta_2^2)$$
$$+\Omega[A_R(\theta_1\dot{\theta}_2-\dot{\theta}_1\theta_2)+C_R(\dot{\theta}_3-\theta_1\dot{\theta}_2)]$$
$$+\tfrac{1}{2}\int(\dot{u}_y^2+\dot{u}_z^2)\,dm_E-R(\dot{\theta}_2\int\dot{u}_z\,dm_E-\dot{\theta}_3\int\dot{u}_y\,dm_E)$$
$$+\dot{\theta}_1\int y\dot{u}_z\,dm_E-\dot{\theta}_2\int x\dot{u}_z\,dm_E+\dot{\theta}_3\int x\dot{u}_y\,dm_E \tag{57}$$

The potential energy depends on spatial derivatives of u_y and u_z. In view of spatial discretization to be adopted shortly, we shall find it advantageous to postpone the discussion of the potential energy.

From Eq. (57), we observe that θ_3 does not appear in the kinetic energy, so that θ_3 is an ignorable coordinate. It follows that

$$\frac{\partial L}{\partial\dot{\theta}_3}=\frac{\partial T}{\partial\dot{\theta}_3}=C\dot{\theta}_3+C_R\Omega+R\int\dot{u}_y\,dm_E+\int x\dot{u}_y\,dm_E$$
$$=\text{const}=C_R\Omega \tag{58}$$

where $L=T-V$ is the Lagrangian and $C_R\Omega$ is recognized as the initial angular momentum about the spin axis. Hence,

$$\dot{\theta}_3=-(1/C)\int(R+x)\dot{u}_y\,dm_E \tag{59}$$

Inserting Eq. (59) into (57), the quadratic part of the kinetic energy becomes

$$T=\tfrac{1}{2}(A\dot{\theta}_1^2+B\dot{\theta}_2^2)+\Omega[A_R-C_R)\theta_1\dot{\theta}_2-A_R\dot{\theta}_1\theta_2]$$
$$-\dot{\theta}_2\int(R+x)\dot{u}_z\,dm_E+\dot{\theta}_1\int y\dot{u}_z\,dm_E$$
$$-\tfrac{1}{2}\Omega^2(C_R-A_R)(\theta_1^2+\theta_2^2)$$
$$-(1/2C)[\int(R+x)\dot{u}_y\,dm_E]^2+\tfrac{1}{2}\int(\dot{u}_y^2+\dot{u}_z^2)\,dm_E \tag{60}$$

At this point, we wish to consider the discretization question. In particular, let us assume that the elastic displacements u_y and u_z can be represented by

$$u_y=\phi_2(P)\zeta_2(t)+\phi_5(P)\zeta_5(t)$$
$$u_z=\phi_1(P)\zeta_1(t)+\phi_3(P)\zeta_3(t)+\phi_4(P)\zeta_4(t)+\phi_6(P)\zeta_6(t) \tag{61}$$

where $\phi_1(P)$ and $\phi_4(P)$ are functions representing the first two out-of-plane bending modes of deformation of the panel, $\phi_2(P)$ and $\phi_5(P)$ represent the first two in-plane bending modes, and $\phi_3(P)$ and $\phi_6(P)$ represent the first two torsional modes, in which P denotes an arbitrary point of the panel. On the other hand, $\zeta_i(t)$ $(i=1,2,..,6)$ are time-dependent generalized coordinates associated with these modes of deformation. It will prove convenient to introduce the following notation:

$$\int(R+x)\phi_i\,dm_E=a_i\qquad \int y\phi_i\,dm_E=b_i$$
$$\int\phi_i\phi_j\,dm_E=m_i\delta_{ij}\qquad (i,j=1,2,...,6) \tag{62}$$

where we note that $a_3=a_6=b_1=b_2=b_4=b_5=0$. Inserting Eqs. (61) and (62) into Eq. (60), we obtain the discretized kinetic energy

$$T=\tfrac{1}{2}(A\dot{\theta}_1^2+B\dot{\theta}_2^2)-\dot{\theta}_2(a_1\dot{\zeta}_1+a_4\dot{\zeta}_4)+\dot{\theta}_1(b_3\dot{\zeta}_3+b_6\dot{\zeta}_6)$$
$$+\tfrac{1}{2}m_1\dot{\zeta}_1^2+\tfrac{1}{2}(m_2-a_2^2/C)\dot{\zeta}_2^2+\tfrac{1}{2}m_3\dot{\zeta}_3^2+\tfrac{1}{2}m_4\dot{\zeta}_4^2$$
$$+\tfrac{1}{2}(m_5-a_5^2/C)\dot{\zeta}_5^2+\tfrac{1}{2}m_6\dot{\zeta}_6^2-(1/C)a_2a_5\dot{\zeta}_2\dot{\zeta}_5$$
$$+\Omega[(A_R-C_R)\theta_1\dot{\theta}_2-A_R\dot{\theta}_1\theta_2]+\tfrac{1}{2}\Omega^2(C_R-A_R)(\theta_1^2+\theta_2^2) \tag{63}$$

The potential energy depends on spatial derivatives of u_y and u_z. Because $\phi_i(i=1,2,...,6)$ represent orthogonal modes of deformation, the potential energy can be written in the form

$$V=\frac{1}{2}\sum_{i=1}^{6}m_i\Lambda_i^2\zeta_i^2 \tag{64}$$

where Λ_i denote the natural frequencies associated with these modes.

Next, let us introduce the configuration vector

$$q=[\theta_1\ \theta_2\ \zeta_1\ \zeta_2\ldots\zeta_6]^T \tag{65}$$

Then, the system Lagrange's equations of motion take the form of Eq. (1), in which the coefficient matrices are

$$m=\left[\begin{array}{c|c}m_{\theta\theta} & m_{\theta\zeta}\\ \hline m^T{}_{\theta\zeta} & m_{\zeta\zeta}\end{array}\right]\quad g=\left[\begin{array}{c|c}g_{\theta\theta} & g_{\theta\zeta}\\ \hline g_{\zeta\theta} & g_{\zeta\zeta}\end{array}\right]\quad k=\left[\begin{array}{c|c}k_{\theta\theta} & k_{\theta\zeta}\\ \hline k^T{}_{\theta\zeta} & k_{\zeta\zeta}\end{array}\right] \tag{66}$$

in which

$$m_{\theta\theta} = \begin{bmatrix} A & 0 \\ 0 & B \end{bmatrix} \qquad m_{\theta\xi} = \begin{bmatrix} 0 & 0 & b_3 & 0 & 0 & b_6 \\ -a_1 & 0 & 0 & -a_4 & 0 & 0 \end{bmatrix}$$

$$m_{\xi\xi} = \begin{bmatrix} m_1 & 0 & 0 & 0 & 0 & 0 \\ 0 & m_2 - a_2^2/C & 0 & 0 & -a_2 a_5/C & 0 \\ 0 & 0 & m_3 & 0 & 0 & 0 \\ 0 & 0 & 0 & m_4 & 0 & 0 \\ 0 & -a_2 a_5/C & 0 & 0 & m_5 - a_5^2/C & 0 \\ 0 & 0 & 0 & 0 & 0 & m_6 \end{bmatrix} \tag{67a}$$

$$g_{\theta\theta} = \Omega(C_R - 2A_R) \begin{bmatrix} 0 & 1 \\ -1 & 0 \end{bmatrix} \quad g_{\theta\xi} = 0 \quad g_{\xi\theta} = 0 \quad g_{\xi\xi} = 0 \tag{67b}$$

$$k_{\theta\theta} = \Omega^2(C_R - A_R) \begin{bmatrix} 1 & 0 \\ 0 & 1 \end{bmatrix} \quad k_{\theta\xi} = 0 \quad k_{\xi\xi} = \text{diag}[m_i \Lambda_i^2] \tag{67c}$$

VII. Numerical Results

The method of analysis presented was applied to the dual-spin configuration shown in Fig. 1. The object is to reduce the oscillation of every component of the state vector x to a tolerable level, where these components consist of the nutation angles θ_1 and θ_2, the amplitudes $\zeta_1, \zeta_2, \ldots, \zeta_6$ of six elastic modes, and the rates $\dot{\theta}_1, \dot{\theta}_2, \dot{\zeta}_1, \dot{\zeta}_2, \ldots, \dot{\zeta}_6$. First, the appendage eigenvalue problem was solved by using the finite-element technique. Two in-plane bending, two out-of-plane bending, and two torsional modes were considered. The lowest three modes were out-of-plane bending, in-plane bending, and twist. The next lowest three modes follow the same order. The computed values of the appendage natural frequencies are

$\Lambda_1 = 2.00418$ rad s^{-1} $\quad \Lambda_4 = 14.27581$ rad s^{-1}
$\Lambda_2 = 3.28803$ rad s^{-1} $\quad \Lambda_5 = 14.38874$ rad s^{-1}
$\Lambda_3 = 5.54724$ rad s^{-1} $\quad \Lambda_6 = 19.16829$ rad s^{-1}

For programming convenience the appendage eigenvalue problem was normalized with respect to the stiffness matrix. Furthermore, the appendage motion was assumed to be antisymmetric. The mass, gyroscopic, and stiffness matrices of the spacecraft were formed by means of Eqs. (67) in which the following parameters were used:

$A_R = 400$ kg-cm^2 $\quad C_R = 2000$ kg-cm^2
$A = 2500$ kg-cm^2 $\quad B = 8000$ kg-cm^2
$\Omega = 2\pi$ rad s^{-1} $\quad C = 12000$ kg-cm^2

The matrices m, g, and k are displayed in Table 1. Next, by using Eqs. (3), the matrices M and G were formed. This permitted the formulation and solution of the eigenvalue problem for the complete spacecraft natural frequencies and the associated eigenvectors. Because this eigenvalue problem is in terms of real symmetric matrices and the order of the problem is relatively small, the Jacobi method was deemed quite adequate for its solution. The first eight spacecraft natural frequencies obtained are

$\omega_1 = 1.66942$ rad s^{-1} $\quad \omega_5 = 8.52519$ rad s^{-1}
$\omega_2 = 3.31079$ rad s^{-1} $\quad \omega_6 = 14.38875$ rad s^{-1}
$\omega_3 = 4.02791$ rad s^{-1} $\quad \omega_7 = 15.20954$ rad s^{-1}
$\omega_4 = 5.91252$ rad s^{-1} $\quad \omega_8 = 19.58347$ rad s^{-1}

For brevity, the modal matrix P is not shown here.

The solution of the eigenvalue problem associated with Eq. (21) and as described in Ref. 6 is only the first step in the spacecraft control. The next step is to simulate the decoupled solution of Eqs. (17) and (20) for proportional and on-off control, respectively. The damping coefficients $2\zeta_r\omega_r$ $(r = 1,2,\ldots,8)$ for proportional control and the deadband constants d_r and control constants k_r $(r = 1,2,\ldots,8)$ for on-off control were chosen so as to drive the system response into tolerable regions within a given time interval. These choices of control parameters do not represent optimal control. Finally, the control loop is closed by designing a decoupled deterministic observer according to Eq. (29). The controller is then actuated by using the estimated coordinates $\hat{\eta}_r(t)$ in conjunction with Eq. (19) for on-off control. Note that the estimated coordinates $\hat{\xi}_r(t)$ are not really needed for control implementation via the observer. A block-diagram for the on-off control system is shown in Fig. 2.

As an illustration, we shall consider the case in which the spacecraft is subjected to an impulsive force at time 0+, while the spacecraft is in equilibrium, $x(0) = \mathbf{0}$. The external excitation vector in Eq. (21) can be written in the form $X(t) = \hat{X}\delta(t)$, where $\hat{X}$ is the magnitude of the generalized impulse vector and $\delta(t)$ is the Dirac delta function. The impulsive force $\hat{X}\delta(t)$ produces an effect on the spacecraft similar to that caused by an initial excitation $x(0+) = M^{-1}\hat{X}$.[8] Note that the effect of meteorite impacts can be simulated in this manner. Hence, we shall consider a system for which $X(t) = \mathbf{0}$ for $t > 0+$ and subjected to the initial

Table 1

$$m = \begin{bmatrix} 2500.0 & 0 & 0 & 0 & 5.290291 & 0 & 0 & -0.634023 \\ & 8000.0 & -54.714107 & 0 & 0 & 1.313164 & 0 & 0 \\ & & 0.497918 & 0 & 0 & 0 & 0 & 0 \\ & & & 0.182460 & 0 & 0 & 0.0000000000088 & 0 \\ & & & & 0.064995 & 0 & 0 & 0 \\ & & \text{symmetric} & & & 0.009814 & 0 & 0 \\ & & & & & & 0.009660 & 0 \\ & & & & & & & 0.005443 \end{bmatrix}$$

$$g = \left[\begin{array}{cc|c} 0 & 7536.0 & 0_{2\times 6} \\ -7536.0 & 0 & \\ \hline \multicolumn{2}{c|}{0_{6\times 2}} & 0_{6\times 6} \end{array}\right] \qquad k = \left[\begin{array}{cc|c} 63101.434634 & 0 & 0_{2\times 6} \\ 0 & 63101.434634 & \\ \hline \multicolumn{2}{c|}{0_{6\times 2}} & 2_{6\times 6} \end{array}\right]$$

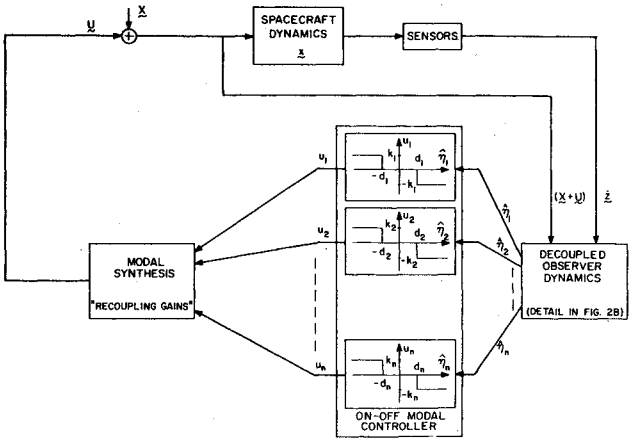

Fig. 2a Control by modal synthesis.

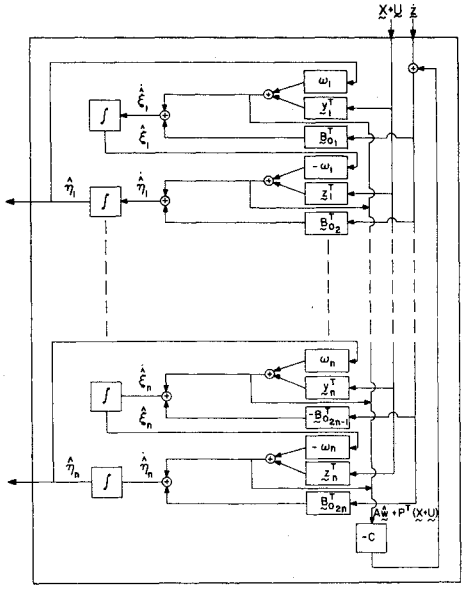

Fig. 2b Decoupled observer.

excitation vector $x(0+)$. Of course, known persistent excitations, such as those due to solar radiation pressure, can be handled separately. Additional details, including numerical values of certain parameters are given in the sequel.

A. Uncontrolled Response

The spacecraft natural frequencies and eigenvectors obtained were used to find the response of the uncontrolled spacecraft with the following initial state vector:

$$x^T(0) = [\dot{\theta}_1 \;\; \dot{\theta}_2 \;\; \dot{\zeta}^T \;\; \theta_1 \;\; \theta_2 \;\; \zeta^T]$$
$$= [10^{-4} \;\; 10^{-4} \;\; 2\times10^{-2} \;\; 0 \;\; 2\times10^{-3}$$
$$2\times10^{-3} \;\; 0 \;\; 2\times10^{-3} \;\; 0 \;\; 0 \;\; 0 \;\; 0 \;\; 0 \;\; 0 \;\; 0]$$

the closed-form solution of the uncontrolled spacecraft can be written as[6]

$$x(t) = \sum_{r=1}^{8} (a_r \cos\omega_r t + b_r \sin\omega_r t)$$

Figures 3a and 3b show in dashed lines the angular velocity $\dot{\theta}_2$ and first out-of-plane elastic coordinate ζ_1 of the uncontrolled spacecraft.

B. Controlled Response

The response of the controlled spacecraft was obtained by using the solutions of the decoupled equations of motion,

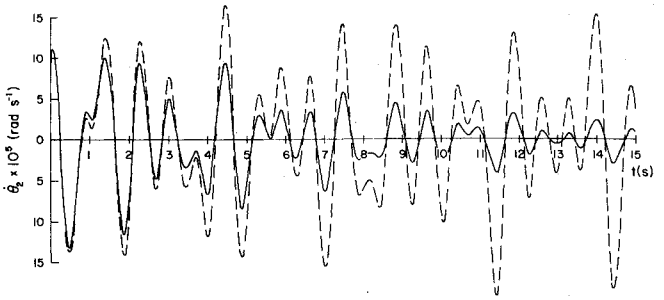

Fig. 3a System response (nutation rate): – – – uncontrolled response, —— response with proportional control.

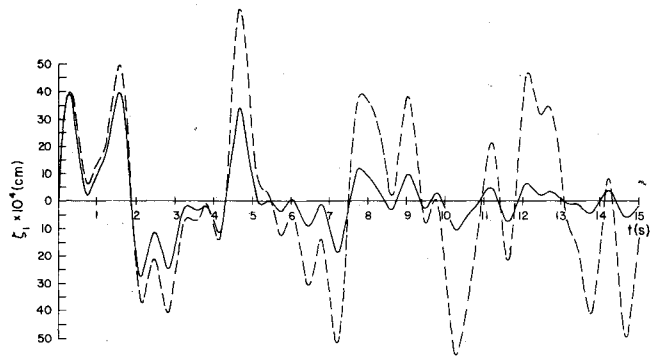

Fig. 3b System response (out-of-plane bending): – – – uncontrolled response, —— response with proportional control.

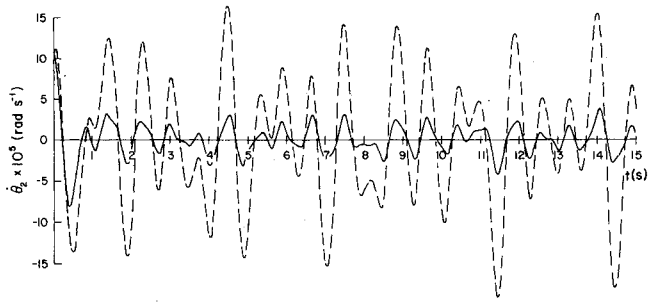

Fig. 4a System response (nutation rate): – – – uncontrolled response, —— response with on-off control.

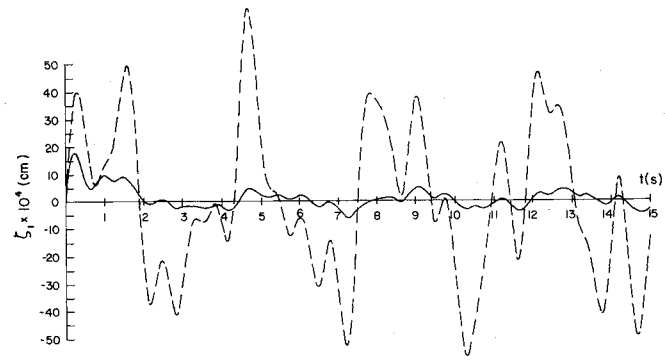

Fig. 4b System response (out-of-plane bending): – – – uncontrolled response, _ _ _ _ response with on-off control.

Eqs. (17) and (20). The solutions yield the decoupled state vector $w(t)$. To obtain the actual state vector $x(t)$, the vector $w(t)$ was premultiplied by the modal matrix P. Figures 3a and 3b show in solid lines the controlled $\dot{\theta}_2$ and the first out-of-plane elastic coordinate ζ_1 of the spacecraft based on a proportional control vector given by Eq. (16). The damping values are $2\zeta_s\omega_s = 0.4$ $(s = 1,...,8)$ and the initial state vector

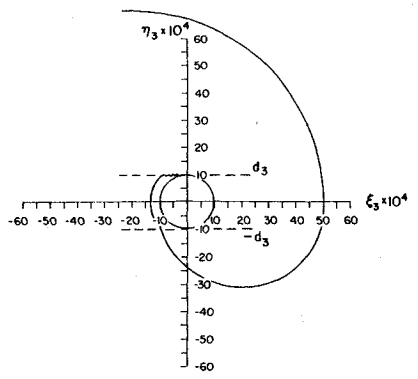

Fig. 5 Typical phase plot of conjugate generalized coordinates.

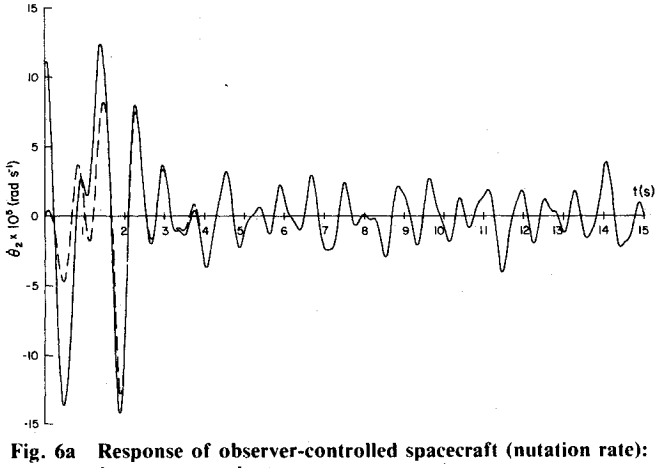

Fig. 6a Response of observer-controlled spacecraft (nutation rate): – – – observer, —— plant.

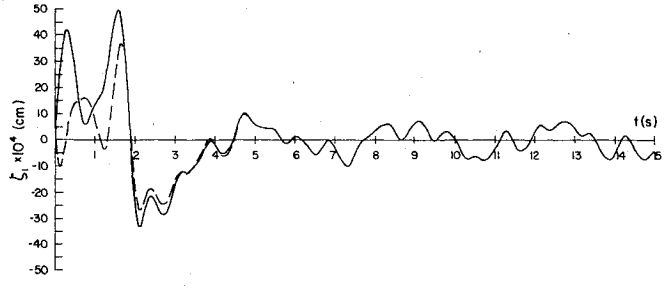

Fig. 6b Response of observer-controlled spacecraft (out-of-plane bending): – – – observer, —— plant.

was the same as that given earlier. Figures 4a and 4b show in solid lines the same angular velocity and elastic coordinate by an on-off scheme of the type given in Eq. (19). For comparison purposes, the uncontrolled response is also shown (see dashed lines). This relay-type control was used on the first five spacecraft modes, leaving the remaining modes uncontrolled with the justification that the amplitudes of these modes were already within the deadband region. The following parameters were used to implement the on-off control:

$$k_r = 0.002\,\omega_r^2 \qquad (r=1,2,3,4)$$

$$k_5 = 0.0005\,\omega_5^2 \qquad k_6 = k_7 = k_8 = 0$$

$$d_r = 0.001 \qquad (r=1,\ldots,8)$$

Figure 5 shows a typical phase plot corresponding to the third pair of conjugate generalized coordinates ξ_3, η_3 for the on-off control.

C. Observer Response

It was assumed that measurements of the nutation rates $\dot{\theta}_1$, $\dot{\theta}_2$ and of the elastic velocity vector $\dot{q}$ were available. Then, using Eqs. (9) and (23), the measurement matrix C for this case becomes

$$C = [0_{n\times n} \mid I_{n\times n}]P$$

A detailed analysis of the measurement process is given in Ref. 11.

The observed coordinates $\hat{\xi}_r$, $\hat{\eta}_r$ $(r=1,\ldots,8)$, i.e., the components of $\hat{w}(t)$ were obtained as a discrete-time solution of Eq. (36). For this purpose, the time interval ΔT was taken to be 0.001 s. The observed state vector $\hat{x}(t)$ was obtained again by premultiplying $\hat{w}(t)$ by the modal matrix P. The eigenvalues of the matrix A_0 were located in the left complex plane at

$$-1.0 \mp 1.8145j \quad -1.0 \mp 3.4585j \quad -1.0 \mp 4.1234j$$

$$-1.0 \mp 6.2511j \quad -1.0 \mp 8.8378j \quad -1.0 \mp 14.4324j$$

$$-1.0 \mp 15.2690j \quad -1.0 \mp 19.6128j$$

D. Control via Observer

Having designed an observer with a satisfactory performance, the spacecraft was controlled by inserting the observer in the control loop. Now that the observer produces the actual generalized coordinates, the on-off control scheme, Eqs. (19), was used with observed $\hat{\eta}_r$ $(r=1,\ldots,8)$ instead of $\eta_r (r=1,\ldots,8)$. Figures 6a and 6b show the coordinates as controlled by the observer.

VIII. Conclusions

The method of control based on modal synthesis is applied to an undamped dual-spin spacecraft exhibiting gyroscopic behavior. Decoupled control has many advantages over standard coupled control. In the first place, it provides a better physical understanding of the system behavior, because it makes it possible to ascertain the degree of participation of each spacecraft mode in the overall system response. It also permits phase-plane representations of the response in terms of conjugate pairs of generalized coordinates. Perhaps more important is the fact that the proposed modal control is very efficient computationally, because it takes advantage of the special nature of the system matrices involved. The Jordan form for the system is a block diagonal matrix with 2×2 blocks involving the spacecraft natural frequencies and is relatively easy to produce. This is in marked contrast to the reduction to Jordan form for general nonsymmetric matrices, which is not computationally feasible for high-order systems. Indeed, the computational advantages of the proposed modal control become more pronounced as the order of the system increases.

The pairs of uncoupled equations are identical in structure, so that the controller design has a modular form consisting of an array of identical units acting in parallel. The method makes it possible to design an observer which is also decoupled into pairs of generalized coordinates.

As an illustration, a dual-spin spacecraft consisting of a rigid rotor and flexible panels is considered. System response for both proportional control and on-off control are presented. A deterministic decoupled observer is designed and inserted in the control loop to control the spacecraft. Control via the observer was done only in conjunction with the nonlinear on-off scheme.

References

[1] Brogan, W.L., *Modern Control Theory*, Quantum Publishers, Inc., New York, 1974.

[2] Simon, J.D. and Mitter, S.K., "A Theory of Modal Control," *Information and Control*, Vol. 13, 1968, pp. 316-353.

[3]Porter, B. and Crossley, T.R., *Modal Control—Theory and Applications*, Taylor & Francis Ltd., London, 1972.

[4]Meirovitch, L., *Analytical Methods in Vibrations*, McGraw-Hill Co., New York, 1967.

[5]Gevarter, W.B., "Basic Relations for Control of Flexible Vehicles," *AIAA Journal*, Vol. 8, April 1970, pp. 666-672.

[6]Meirovitch, L., "A New Method of Solution of the Eigenvalue Problem for Gyroscopic Systems," *AIAA Journal*, Vol. 12, Oct. 1974, pp. 1337-1342.

[7]Meirovitch, L., "A New Method of Solution of the Eigenvalue Problem for Gyroscopic Systems," *Journal of Applied Mechanics*, Vol. 12, Oct. 1974, pp. 1337-1342.

[8]Meirovitch, L., VanLandingham, H.F., and Öz, H., "Control of Spinning Flexible Spaceraft by Modal Synthesis," Paper No. 76-022, XXVIIth International Astronautical Congress of the I.A.F., Anaheim, Calif., Oct. 10-16, 1976, also *Acta Astronautica*, Vol. 4, 1977, pp. 985-1010.

[9]Meirovitch, L. and Öz, H., "Modal Control of Distributed Gyroscopic System," AIAA Paper 78-1421, AIAA/AAS Astrodynamics Conference, Palo Alto, Calif., Aug. 7-9, 1978.

[10]Luenberger, D.G., "An Introduction to Observers," *IEEE Transactions on Automatic Control*, Vol. AC-16, Dec. 1971, pp. 596-602.

[11]Meirovitch, L., Van Landingham, H.F., and Öz, H., "Distributed Control of Spinning Flexible Spacecraft," *Proceedings AIAA Symposium on Dynamics and Control of Large Flexible Spacecraft*, Blacksburg, Va., June 13-15, 1977, pp. 249-269.